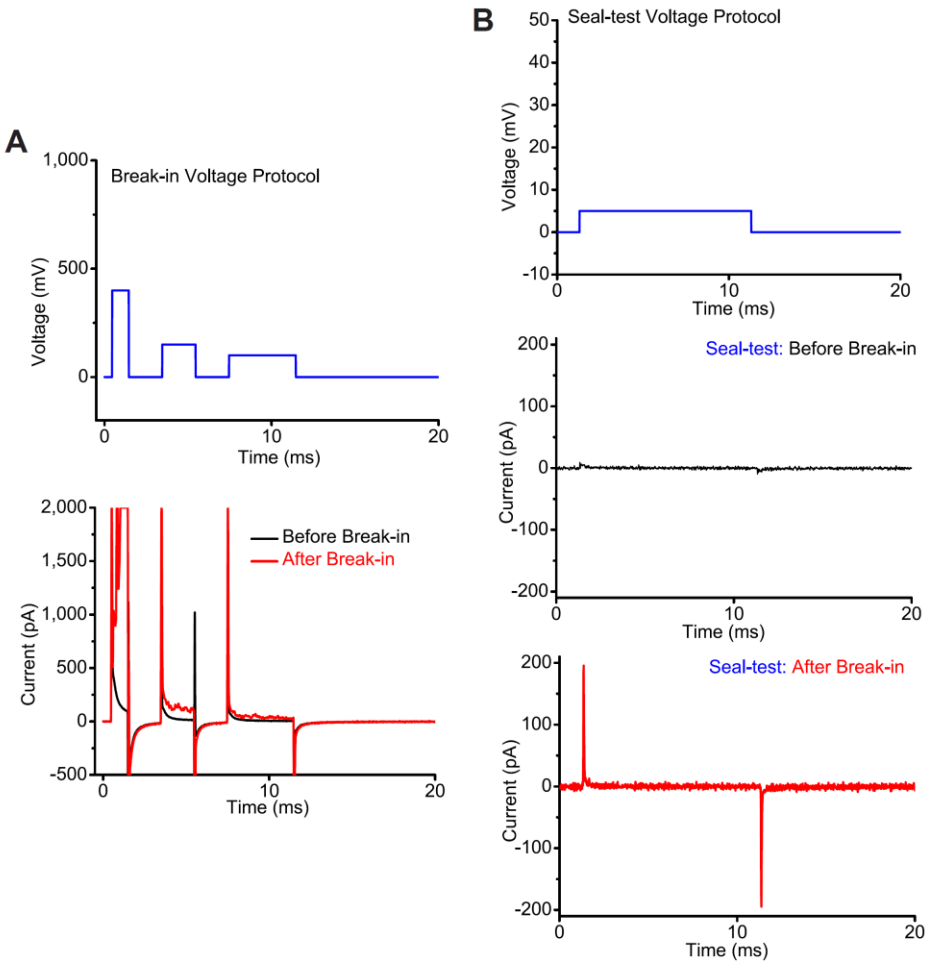

Figure S1. Experimental protocols for the whole-endolysosome patch-clamp technique--Related to Figure 1.

(A). Membrane test (the lower panel) before (black) and after (red) break-in using a voltage protocol (upper panel).

(B). Membrane test before (middle panel, black) and after (lower panel, red) break-in using a seal-test voltage protocol (upper panel).

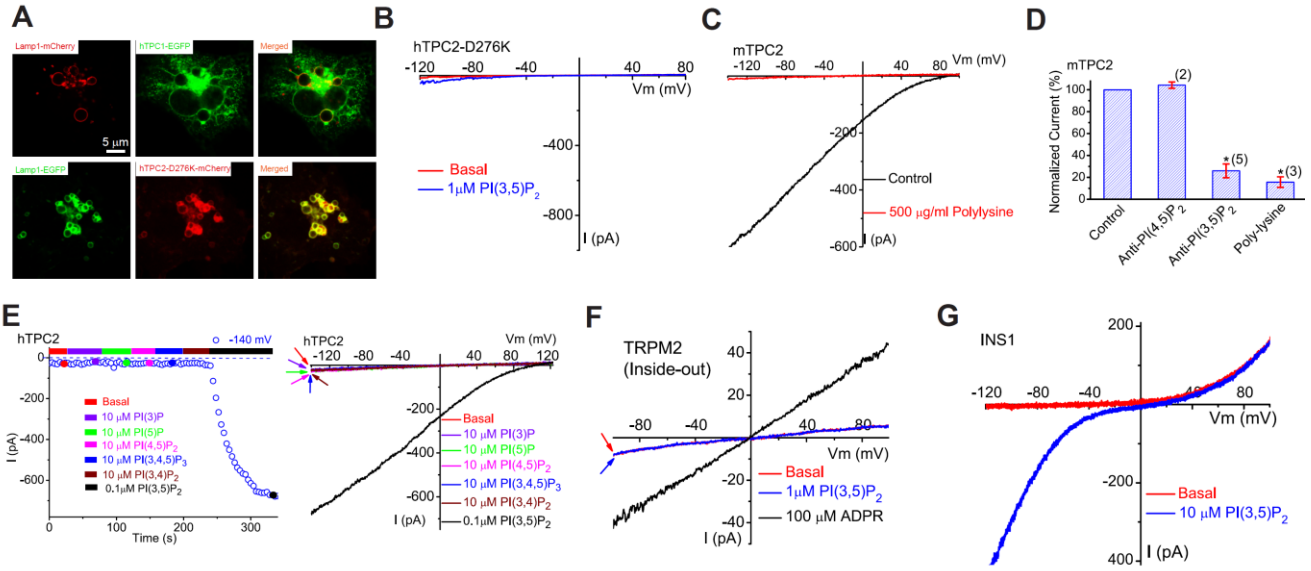

Figure S2. $PI(3,5)P_2$ activates recombinant TPCs in endolysosomes--Related to Figure 2.

(A). Human TPC1 and TPC2 pore-mutant proteins were localized in endosomes and lysosomes. COS-1 cells were transfected with TPC and Lamp-1 fusion proteins and treated with vacuolin-1.

(B). A mutation of a negatively-charged amino acid residue in the first putative pore region of TPC2 abolishes I_{hTPC2}. $PI(3,5)P_2$ (1 μM) activated a small TRPML-like current, but not I_{hTPC2}, in an enlarged endolysosome/vacuole isolated from an *hTPC2-D276K*-transfected COS-1 cell.

(C). $PI(3,5)P_2$ –activated I_{mTPC2} was inhibited by bath (cytoplasmic) application of poly-L-lysine (500 μg/ml) to an enlarged endolysosome isolated from an mTPC2-EGFP-expressing COS-1 cell.

(D). I_{mTPC2} (post $PI(3,5)P_2$ application) was inhibited 80- 90% by bath application of poly-L-lysine (500 μg/ml) or anti-$PI(3,5)P_2$ antibody (5 μg/ml). The inhibition was irreversible (within several minutes), but I_{mTPC2} could be re-activated by $PI(3,5)P_2$ upon washout of poly-L-lysine or anti-$PI(3,5)P_2$ antibody.

(E). Specific activation of hTPC2 by $PI(3,5)P_2$ (in 0.1 μM), but not other diC8 PIPs (all in 10 μM). The right panel shows representative traces of I_{hTPC2} with different PIPs applied at different time points, as shown in the left panel.

(F). Bath application of ADPR (100 μM), but not $PI(3,5)P_2$ (1 μM), activated a current with a linear I-V in an inside-out patch excised from a TRPM2-transfected HEK293T cell.

(G). $PI(3,5)P_2$ (10 μM) selectively activated the inward, but not the outward current, in an endolysosome isolated from an INS1 pancreatic β-cell.

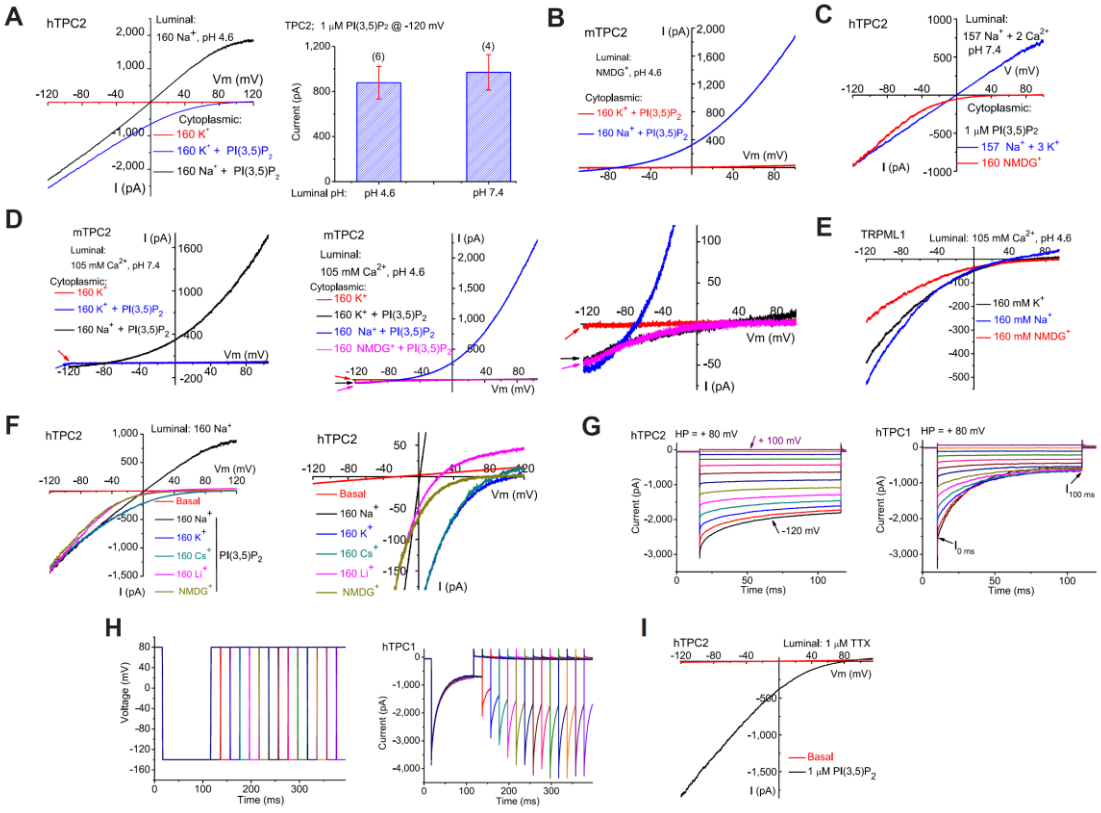

Figure S3. Whole-endolysosome I_{hTPC2} is selective for Na^+--Related to Figure 3.

(A). I_{TPC2} is selective for Na^+ over K^+ at both acidic and neutral luminal pH. Left panel: large outward I_{hTPC2} was seen with cytoplasmic Na^+, but not K^+, in the presence of luminal Na^+ at low pH (pH 4.6); Right panel: the current amplitudes of $PI(3,5)P_2$-activated I_{TPC2} were similar at neutral and acidic luminal pH.

(B). I_{mTPC2} is impermeant to $NMDG^+$ or H^+; I_{mTPC2} exhibited no significant inward current in the presence of luminal $NMDG^+$ (150 mM; pH4.6), and cytoplasmic K^+ (160 mM) or Na^+ (160 mM).

(C). Little or no effect of luminal Ca^{2+} on the inward current and E_{rev} of I_{hTPC2}.

(D). I_{mTPC2} is selective for Na^+ over Ca^{2+} at acidic and neutral luminal pH. Left panel: in luminal isotonic Ca^{2+} (105 mM; pH 7.4) and cytoplasmic Na^+, E_{rev} for I_{hTPC2} was < -60mV. Middle and right (an expanded view) panels: low I_{mTPC2} permeability to luminal Ca^{2+} under bi-ionic conditions (luminal isotonic Ca^{2+} versus cytoplasmic Na^+), the E_{rev} of I_{TPC2} was -68 ± 2mV (n = 12).

(E). I_{TRPML1} is highly Ca^{2+}-permeable; I_{TRPML1} with luminal isotonic Ca^{2+} and cytoplasmic Na^+ or K^+ exhibited a positive E_{rev} (**+** 47 ± 2mV, n = 3**).**

(F). I_{hTPC2} is selectively permeable to Na^+, and to a lesser degree Li^+, but not K^+ or Cs^+; I_{hTPC2} was recorded in the presence of cytoplasmic monovalent cations and luminal Na^+. Right panel shows an expanded view of E_{rev} in the presence of different cytoplasmic monovalent cations.

(G). I_{hTPC2} and I_{hTPC1} elicited by a voltage-step protocol. HP = + 80 mV.

(H). Time-dependent recovery of I_{TPC1} from inactivation at negative voltages. Removal of voltage-dependent inactivation (at -140 mV) by a short pre-pulse to positive membrane potential (+ 80 mV). Right panel shows the voltage protocol used to study the time-dependent recovery of I_{hTPC1} from inactivation.

(I). Insensitivity of I_{hTPC2} to TTX (included in the luminal/pipette solution; pH 7.4).

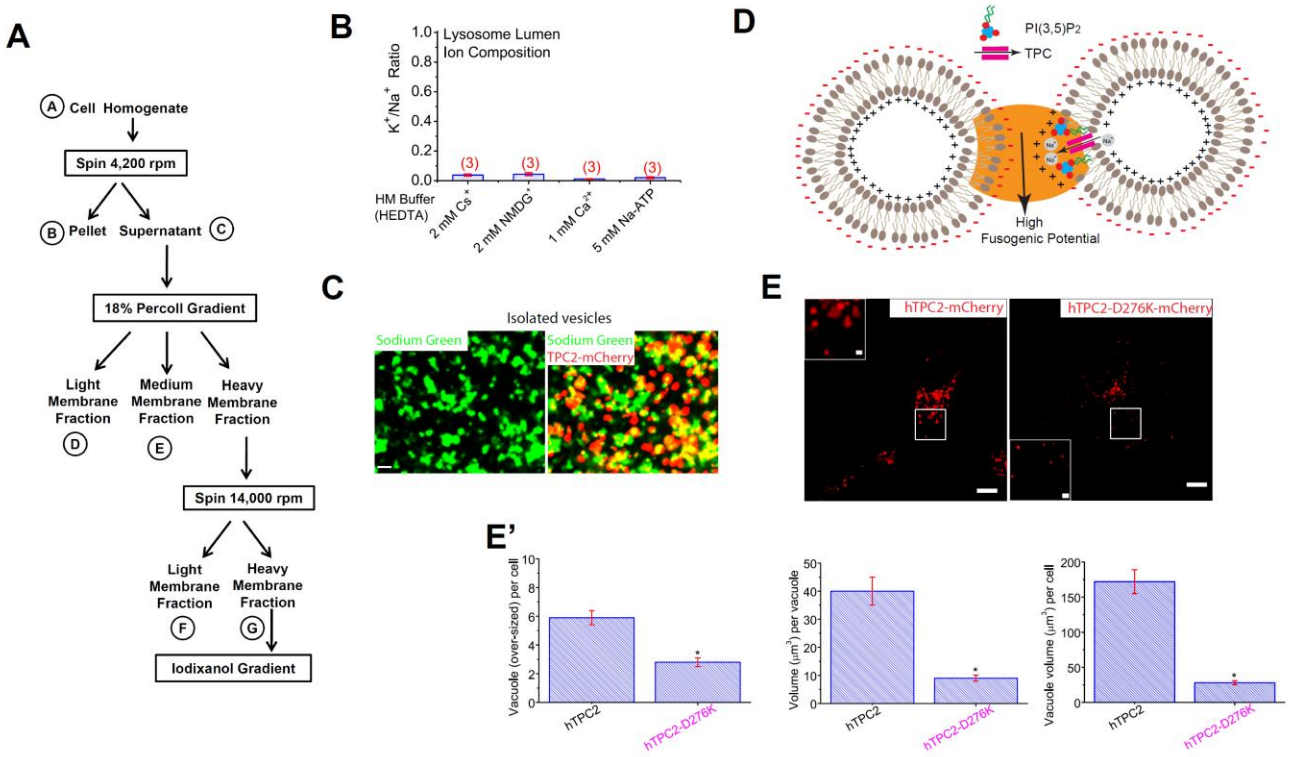

Figure S4. Ionic composition in the lysosomes of HEK293T cells isolated by cellular fractionation--Related to Figure 4.

(A). Centrifugation of cell homogenate (fraction A) of HEK293T cells resulted in a pellet (fraction B) and a supernatant (fraction C). The supernatant was then layered over a discontinued gradient containing a cushion of 2.5 M sucrose and 18% Percoll in the HM buffer. Further centrifugation of the gradient resulted in the light membrane fraction (fraction D), the medium membrane fraction (fraction E), and the heavy membrane fraction (fraction G).

(B). Luminal K^+/Na^+ ratios under various homogenizing buffer conditions.

(C). TPC2-mCherry-positive isolated vesicles/lysosomes were loaded with Sodium Green dye. Scale bar = 2 μm**.**

(D). An electrostatic model for the potential role of TPC-mediated Na^+ flux in endolysosomal dynamics. Endolysosomes have a luminal-side positive transmembrane potential at rest (estimated to be + 30 to + 110 mV; see ref. (Dong et al., 2010)). Charge repulsion may prevent docking and fusion of alike endolysosomes. Upon PIKfyve recruitment/activation, rapid and localized generation of $PI(3,5)P_2$ triggers TPC-mediated Na^+ efflux and subsequent depolarization of the endolysosomal membrane toward E_{Na}. This rapid and localized reversal of charge may permit the fusion of the $PI(3,5)P_2$-enriched microdomain.

(E). Vacuole size measurement in COS1 cells transfected with either hTPC2-mCherry or hTPC2-D276K-mCherry constructs. Images were taken using an Olympus Spinning-Disk confocal with 0.2 μm Z-steps. Vacuole size was measured using the 4D viewer and object measurement functions of Metamorph (Olympus) software. Scale bar = 10 μm (2 μm for the inset). **(E').** Over-sized vacuoles (radius > 1 μm) were analyzed for number of vacuoles per cell, volume per vacuole, and total vacuole volume/cell. For each group, cells (n =49) were randomly selected from 3 independent transfections.

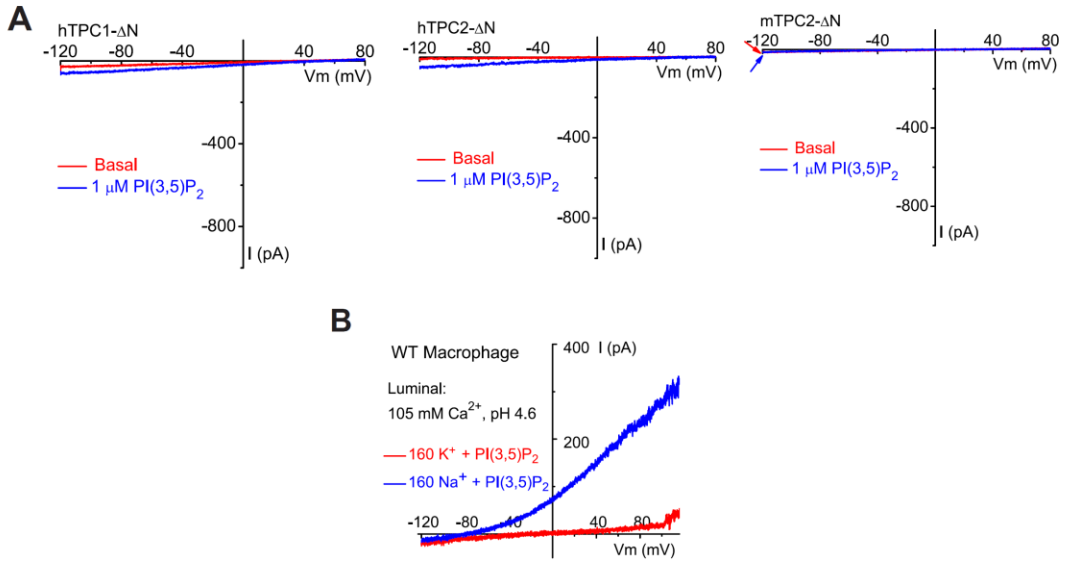

Figure S5. N-terminal truncations of TPC1 and TPC2 abolish TPC currents in the endolysosome--Related to Figure 5.

(A). N terminal truncations in hTPC1, hTPC2, and mTPC2 abolished I_{TPC}. $PI(3,5)P_2$ (1 μM) activated small currents in enlarged vacuoles isolated from hTPC1-ΔN (the left panel), hTPC2-ΔN (the middle panel), or mTPC2-ΔN (the right panel) -transfected COS-1 cells**.**

(B). $PI(3,5)P_2$ –activated whole-endolysosome currents in macrophages are Na^+ selective over Ca^{2+}. E_{rev} was negative for an endogenous whole-endolysosome $PI(3,5)P_2$-activated current of a macrophage in the presence of luminal isotonic Ca^{2+} and cytoplasmic Na^+.

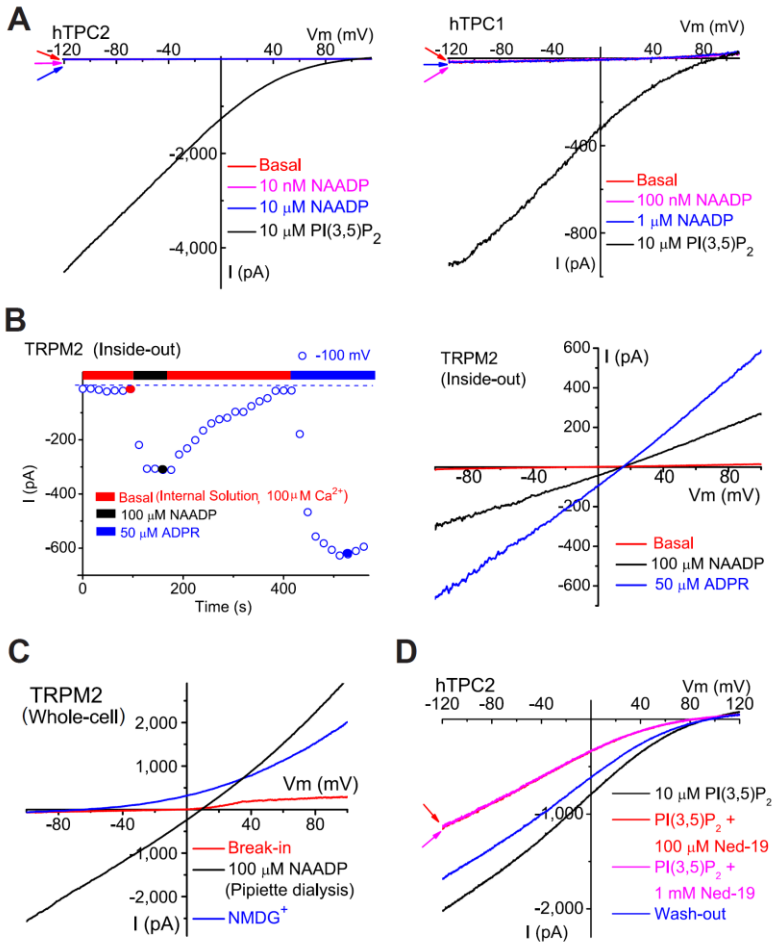

Figure S6. NAADP activates TRPM2, but not TPC1 or TPC2--Related to Figure 6.
(A). NAADP (10 nM or 10 μM) failed to activate whole-endolysosome I_{hTPC2}. In contrast, $PI(3,5)P_2$ robustly activated I_{hTPC2} in the same vacuole. Likewise, NAADP (100 nM or 1 μM) failed to activate whole-endolysosome I_{hTPC1}. In contrast, $PI(3,5)P_2$ robustly activated I_{hTPC1} in the same vacuole.
(B). NAADP (100 μM) or ADPR (50 μM) activated a current with a linear I-V in an inside-out patch excised from a TRPM2-transfected HEK293T cell.
(C). Activation of whole-cell I_{TRPM2} by pipette dialysis of NAADP. Inclusion of NAADP (100 μM) into the pipette solution under the whole-cell configuration induced I_{TRPM2} in a TRPM2-transfected HEK293T cell.
(D). I_{hTPC2} was relatively insensitive to Ned-19, a blocker of the endogenous NAADP receptor; $PI(3,5)P_2$-activated I_{hTPC2} was weakly inhibited by Ned-19 (100 μM or 1mM).

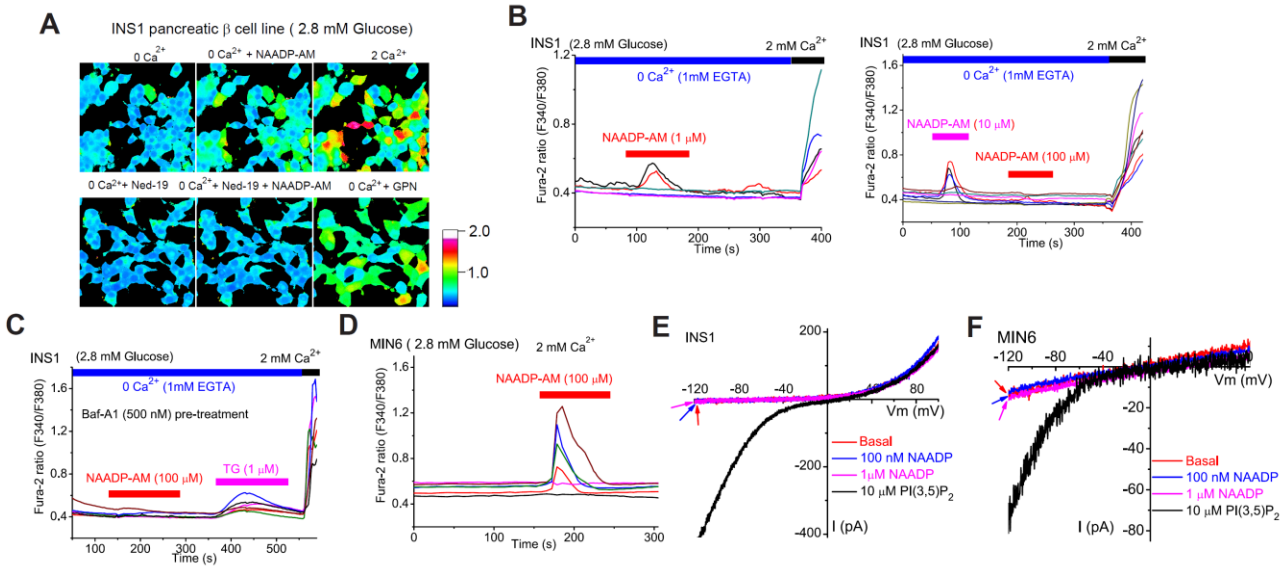

Figure S7. Pancreatic β-cell lines exhibit NAADP-induced lysosomal Ca^{2+} release but lack TPC currents--Related to Figure 7.

(A). In the absence of external Ca^{2+} (free [Ca^{2+}] < 10 nM), NAADP-AM (100 μM) induced Ca^{2+} release measured with Fura-2 (F_{340}/F_{380}) ratios from intracellular stores in INS1 cells. Ned-19 (50 μM) abolished the majority of the response.

(B). NAADP-AM (1 μM) induced small Ca^{2+} transients in a subset of INS1 cells in the absence of external Ca^{2+} ('0' Ca^{2+}); NAADP-AM (10 μM) induced and desensitized Ca^{2+} release in INS1 cells. After NAADP-AM (10 μM) induced small Ca^{2+} transients in a subset of INS1 cells in the absence of external Ca^{2+} ('0' Ca^{2+}), a higher concentration of NAADP-AM (100 μM) failed to further induce Ca^{2+} responses in the same cells.

(C). Bafilomycin A1 pretreatment abolished NAADP-induced Ca^{2+} release in INS1 cells; thapsigargin (TG; 1 μM) induced Ca^{2+} responses in the same cells.

(D). NAADP-AM (100 μM) induced small Ca^{2+} transients in MIN6 pancreatic β-cells.

(E). NAADP (100 nM or 1 μM) failed to elicit whole-endolysosome current in INS1 cells. In contrast, $PI(3,5)P_2$ activated TRPML-like currents (re-plotted from the *Suppl. Fig. S2G*) in the same vacuole. Note that the outward current present in this vacuole was insensitive to $PI(3,5)P_2$.

(F). $PI(3,5)P_2$ activated predominantly TRPML-like inward currents in MIN6 cells. NAADP (100 nM or 1 μM) failed to elicit any measureable whole-endolysosome current in MIN6 cells. In contrast, $PI(3,5)P_2$ activated TRPML-like currents in the same vacuole.